Water Resources Research

Supporting Information for

Challenges and Capabilities in Estimating Snow Mass Intercepted in Conifer Canopies with Tree Sway Monitoring

Mark S. Raleigh[1], Ethan D. Gutmann[2], John T. Van Stan II[3], Sean Burns[2,4], Peter Blanken[4], and Eric E. Small[5]

[1]College of Earth, Ocean, and Atmospheric Sciences, Oregon State University, Corvallis, OR, USA.

[2]National Center for Atmospheric Research, Boulder, CO, USA.

[3]Department of Biological, Geological, and Environmental Sciences, Cleveland State University, Cleveland, OH, USA.

[4]Department of Geography, University of Colorado, Boulder, CO, USA.

[5]Department of Geological Sciences, University of Colorado, Boulder, CO, USA.

Contents of this file

Introduction

This supporting information document includes additional details on (1) the accelerometer installation and study trees, (2) the dependence of tree sway on temperature and the independence of tree sway from wind speed, (3) the effect of window size on derived tree sway frequency, (4) the estimation of thermal effects on tree sway with different temperature datasets, and (5) the conversion of changes in tree sway to changes in mass.

Text S1. Additional details on accelerometer installation

The Gulf Coast Data Concepts (GCDC) accelerometers were weatherproofed in plastic wrap and installed on the north side of each study tree. Magnetic north was used as the reference using a compass, though the sensors were not precisely oriented to north. The USB port of each GCDC sensor was oriented toward the ground. Given this configuration, the sensor "X-axis" was the vertical axis, while the "Y-axis" (east-west motion) and "Z-axis" (north-south motion) were the lateral axes (see GCDC X16-1D user manual, dated March 22, 2016, available at http://www.gcdataconcepts.com/GCDC_X16-1D_User_Manual.pdf). The installation height and basic tree measurements are shown in Table S1.

For each GCDC accelerometer, data were stored on an internal memory card and were downloaded manually by unplugging the USB cable from the power supply at the access port (Fig. 3c in main text) and connecting to a field laptop. After download, the memory card was cleared, the time/date corrected for drift (typically negligible), and the USB was reconnected to the power source to resume data logging.

The GCDC accelerometer has an on-board AA battery (Fig. 3a in main text), which was insufficient to ensure long-term monitoring of tree sway. We provided external power from a nearby datalogger to each accelerometer via the USB extension and a 12V to 5V USB DC Converter (manufacturer: Autotek).

Text S2. Comparisons of seasonal temperature and wind speed to tree sway

Time series of hourly air temperature (Figure S1), bole temperature (Figures S2-S3), and wind speed (Figure S4) are included for additional interpretation of the tree sway time series (Figure 6 in main text). A direct comparison of tree sway versus air temperature and wind speed is shown in Figure S5. This illustrates the seasonality of tree sway with higher sway frequency at lower temperatures (typically in the winter months) and lower sway frequency at higher temperatures (typically in the summer months) (Fig. S5a,c).

In contrast to temperature, wind speed shows lower correspondence to the sway frequency data (Fig. S5b,d). A given wind speed may yield wide range of sway frequency values, which reinforces that sway frequency does not depend on the magnitude of wind speed but rather on tree properties related to mass, rigidity, and geometry (see Equation 1 in main text). Although lower sway frequency and wind speeds are found in summer, and higher sway frequency and higher wind speeds are found in winter, the relationship is not casual. The main dependence on observed tree sway frequency and wind speed is that there appears to be a threshold wind speed required to induce tree movement (note gap at the left side of the data near 0 m s^{-1} in Fig. S5b,d). For the spruce tree, 99% of the detected tree sway values had a mean hourly wind speed of at least 1.26 m s^{-1}, while 99.9% had a mean hourly wind speed of at least 0.56 m s^{-1}. For the fir tree, 99% of the detected tree sway values had a mean hourly wind speed of at least 0.96 m s^{-1}, while 99.9% had a mean hourly wind speed of at least 0.26 m s^{-1}. The tree-to-tree differences in these wind speed thresholds necessary to initiate sway motion may be due to the difference in tree size (i.e., the spruce is larger and may require higher wind speed to set into motion).

Although the tree sway frequency does not depend on wind speed (assuming it is above the threshold for movement initiation), the variations in hourly tree movement scale directly with

wind energy (Figure S6 and Figure 4a in main text). Here, the variations in tree movement are characterized with the standard deviation in lateral acceleration, while wind energy is the squared wind speed. A higher squared wind speed causes greater variations in tree motion (i.e., more chaotic), which should be readily understood. This figure is tangential to the main analysis (which focuses on tree sway frequency, not the standard deviation in tree acceleration), but is included to convey the manner in which tree motion responds to wind speed.

Text S3. Selection of window length for frequency analysis

In the main analysis, we conducted frequency analysis on the 12 Hz accelerometer data to identify a sway frequency over a window length of 1 hour (60 minutes). We tested whether selection of a narrower window (5 minutes) would significantly alter the analysis. For this analysis, we only present data from one lateral axis on the spruce tree over mid-winter in water year 2017 (Figures S7-S8). Similar tree sway values were found for both window sizes (5 minute and 60 minute), but the 5-minute window produced additional noise at short time scales and sporadic larger variations from the prevailing values. We did not assess the mechanism behind these sporadic deviations in 5-minute tree sway. The sway values were in close agreement (Figure S8), regardless of whether a 60-minute window was used for the frequency analysis or a 5-minute window was used (and all 5-minute values averaged to a 60-minute value). These comparisons supported our selection of a 60-minute window for the main frequency analysis, as it reduced noise relative to the 5-minute window, while yielding similar central values.

Text S4. Estimation of unloaded sway with tree bole temperature versus air temperature

We fit Equation 4 (see main text) to a subset of points (n=1000) when snow was known to be absent from the forest canopy. This fit was done separately for each water year to control for changes in sway frequency due to tree growth. In developing the fit, we evaluated use of both hourly bole temperatures and 36-hour smoothed air temperatures. The fit of Equation 4 for each year, temperature dataset, and tree are shown in Figures S9-S10. The derived parameters and fit statistics are shown in Tables S2-S3. Similar skill metrics were achieved regardless of which temperature dataset was used to fit the model. For the spruce tree, the bole temperature yielded improved statistics in three out of the five water years when both temperature datasets were available. For the fir tree, the air temperature yielded improved statistics in four out of the five years. The standard deviation in the residuals of the fit varied with temperature (Figure S11), which was accounted for in the calculation of the signal-to-noise (SNR) threshold used to detect the snow interception signal (see main text).

Text S5. Estimation of changes in mass from changes in tree sway

Sway tests were used to determine the slope parameter in Equation 7 (see main text) for each tree. The fitted parameter (with 95% confidence intervals) and statistics are shown in Table S4. Note that the equation assumes linearity and that the largest snow masses intercepted in the canopy exceeded the upper limit of masses used in the sway tests. Additionally, the sway tests were conducted with mass at only a single height near the accelerometer (Table S1).

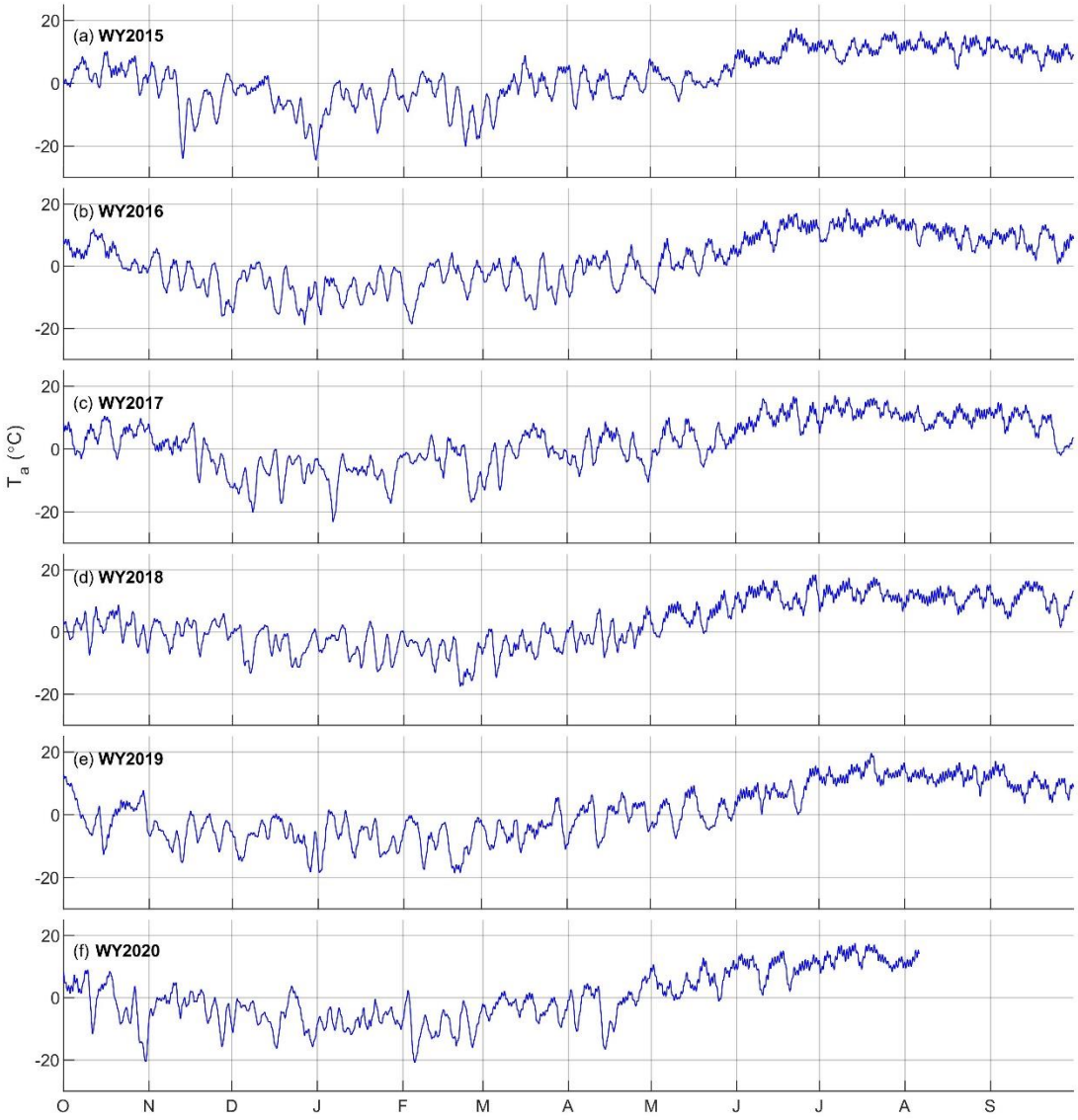

Figure S1. Hourly air temperature (36-hour smoothed) measured at 8m height on the US-NR1 AmeriFlux tower over water years (WY) 2015-2020.

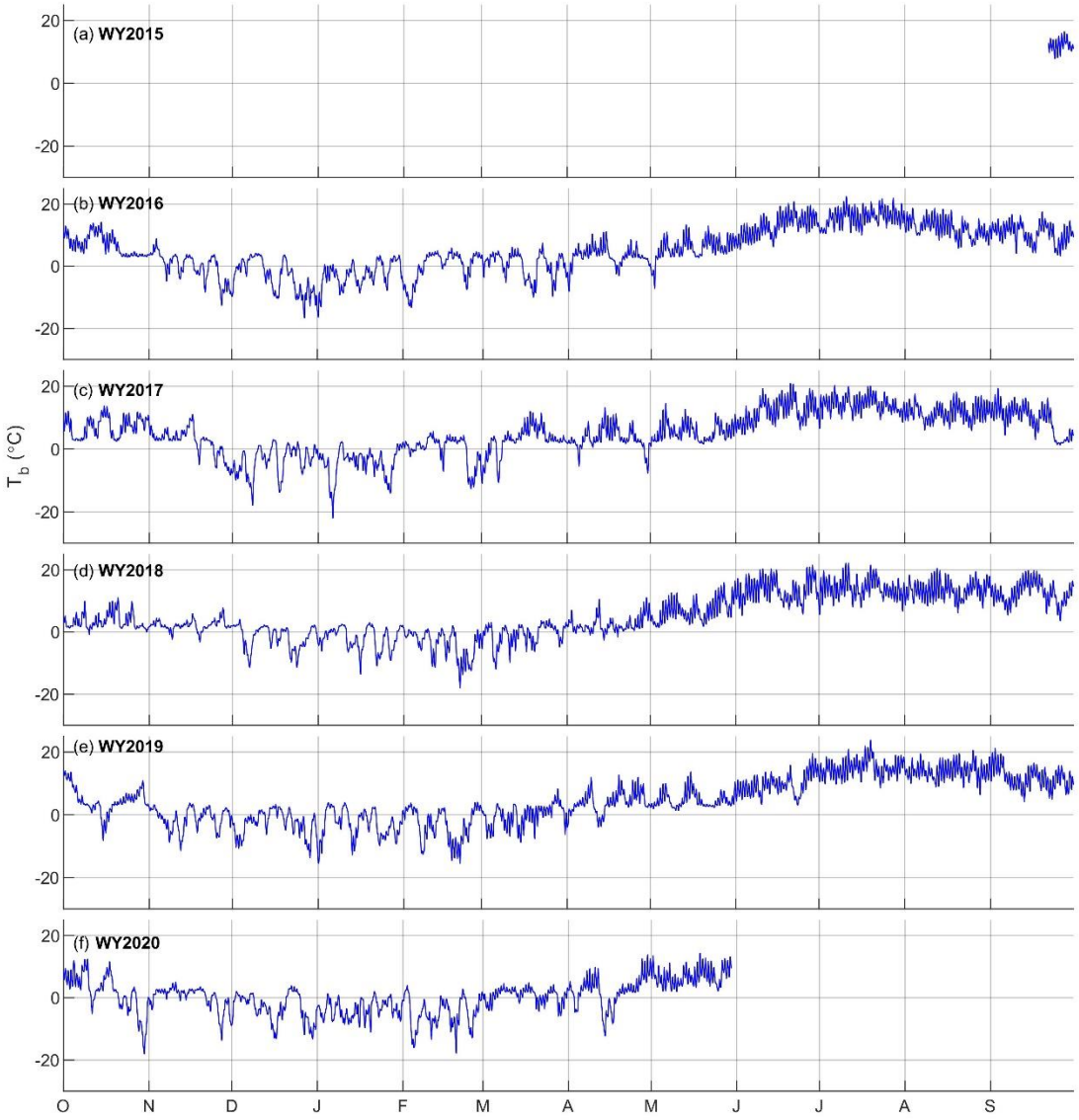

Figure S2. Hourly tree bole temperature from a spruce tree near the US-NR1 AmeriFlux tower over water years (WY) 2015-2020.

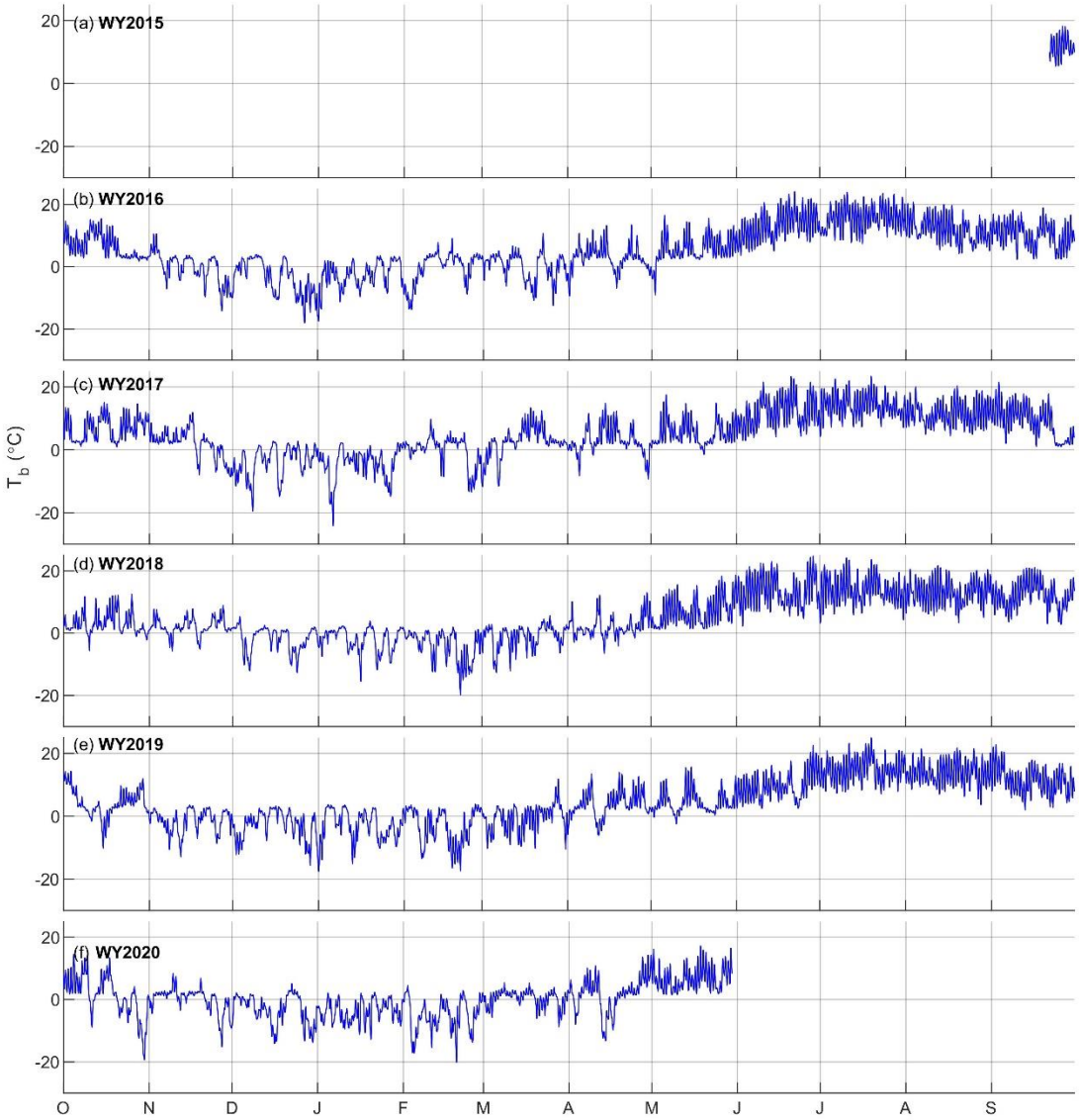

127

128 **Figure S3.** Hourly tree bole temperature from a fir tree near the US-NR1 AmeriFlux tower over
129 water years (WY) 2015-2020.

130

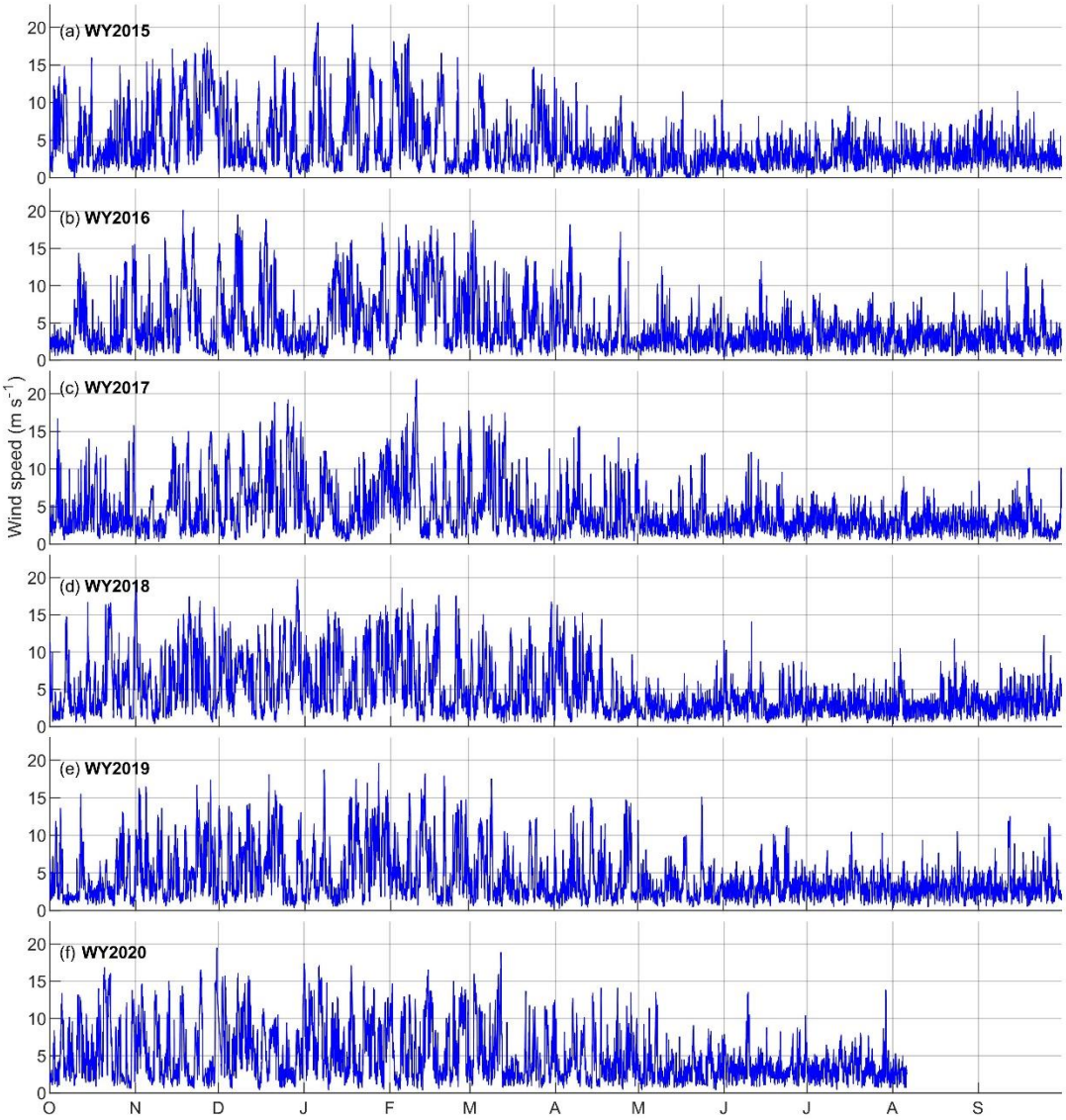

131

132 **Figure S4.** Hourly wind speed measured at 21m height on the US-NR1 AmeriFlux tower over
133 water years (WY) 2015-2020.

134

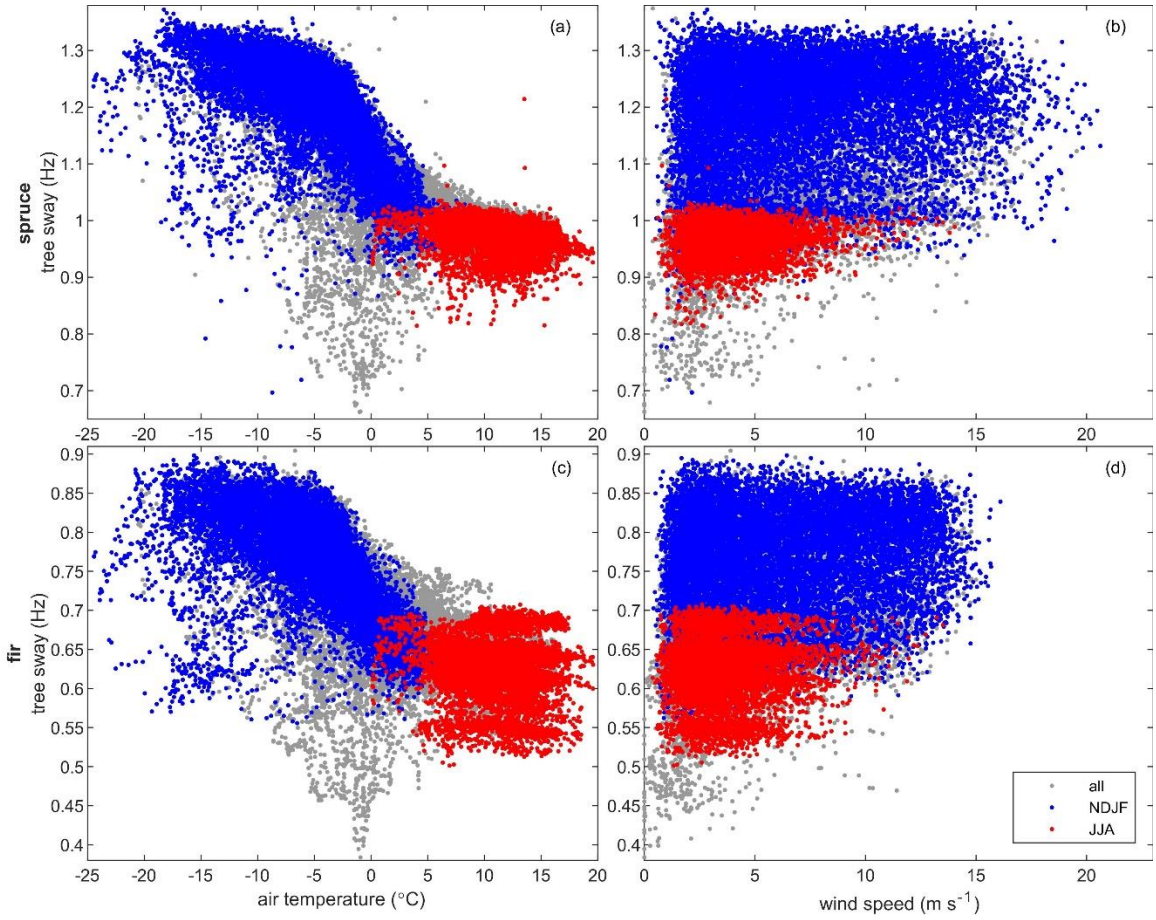

Figure S5. Comparison of hourly observations of tree sway and (left) air temperature (smoothed over 36 hour window) and (right) wind speed for the (top) spruce and (bottom) fir with all data shown in the study period (November 2014 – August 2020). Points are colored blue for winter months (November-February, NDHF) and red for summer months (June-August, JJA). This figure shows that tree sway frequency varies with temperature but is independent of wind speed. The tree sway data are from the east-west axis, and after filtering but before smoothing in time.

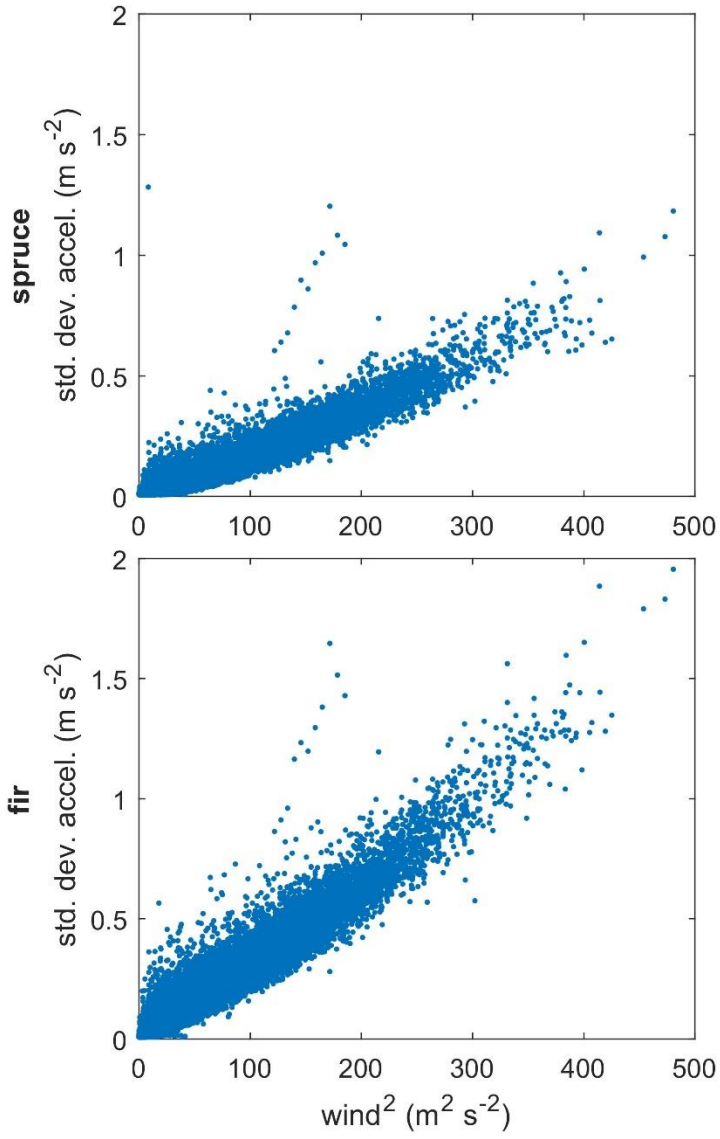

144

145 **Figure S6.** Comparison of hourly values of squared wind speed versus standard deviation in
146 lateral tree acceleration for the (a) spruce and (b) fir over the study period (November 2014 –
147 August 2020). The acceleration data are from the east-west axis.

148

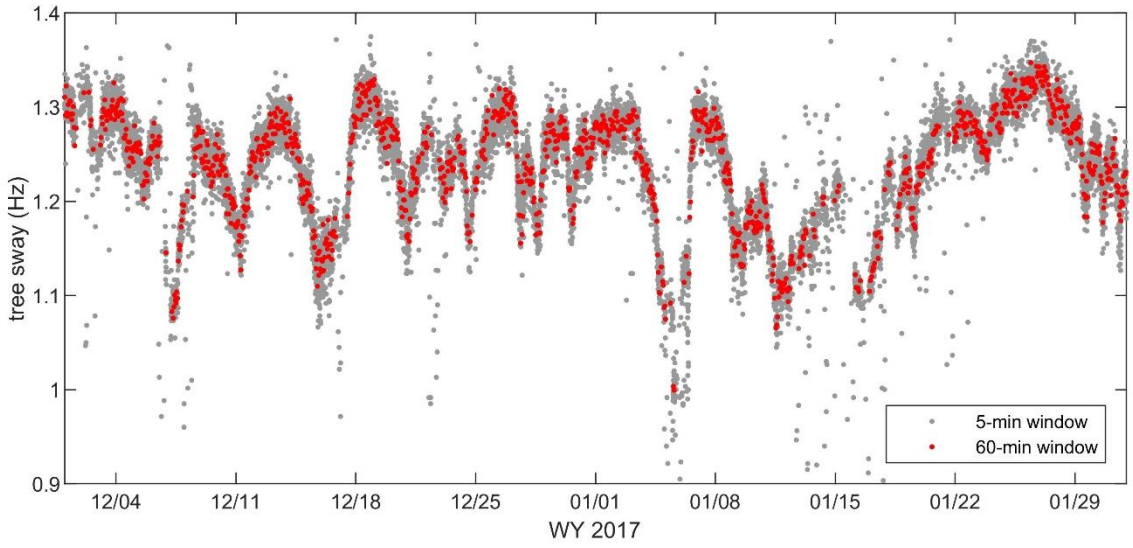

Figure S7. Time series of tree sway derived from acceleration data using a 60-minute window (red dots) versus a 5-minute window (gray dots). Example data shown are from the east-west axis of the spruce tree in December-January in water year (WY) 2017. The analysis in the main text used a 60-minute window (i.e., hourly).

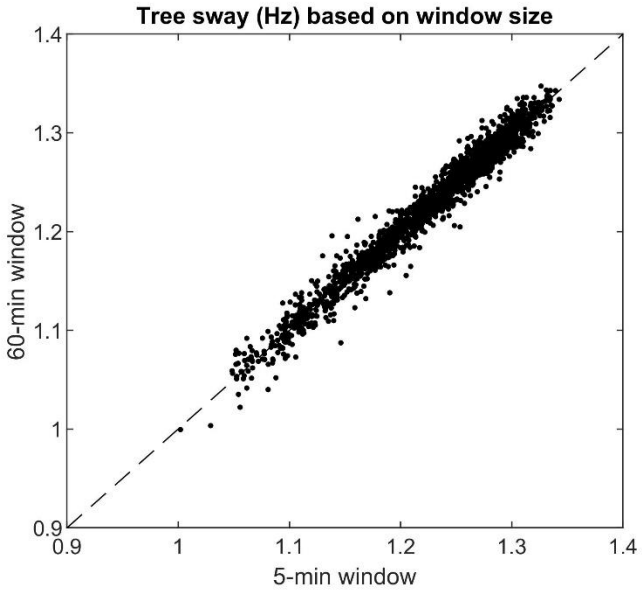

Figure S8. Scatterplot of tree sway derived from acceleration data using a 60-minute window versus a 5-minute window. All 5-minute sway values in each 60-minute period are averaged to facilitate the comparison. Example data are from the east-west axis of the spruce tree in from late November to early March in water year (WY) 2017.

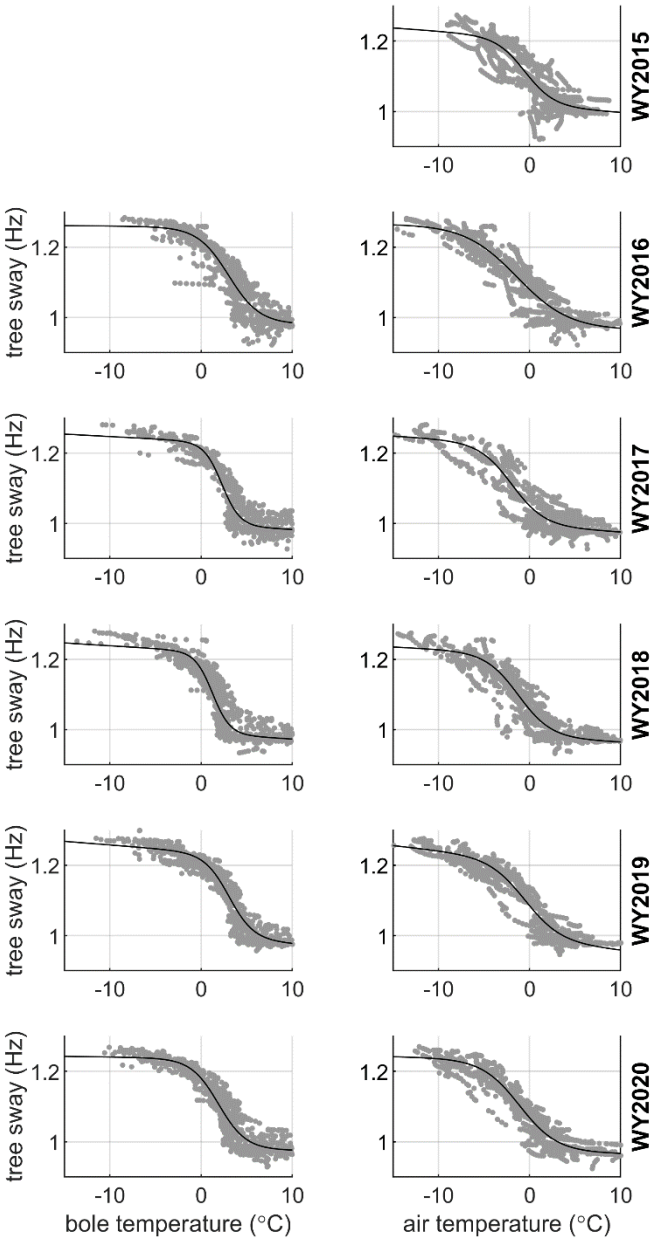

Figure S9. Hourly observed tree sway frequency versus (left) bole temperatures and (right) 36-hr smoothed air temperatures across the six water years (rows), for the Niwot spruce tree. The gray markers are the points (n=1000) used to fit the model (black line, Equation 4 in main text).

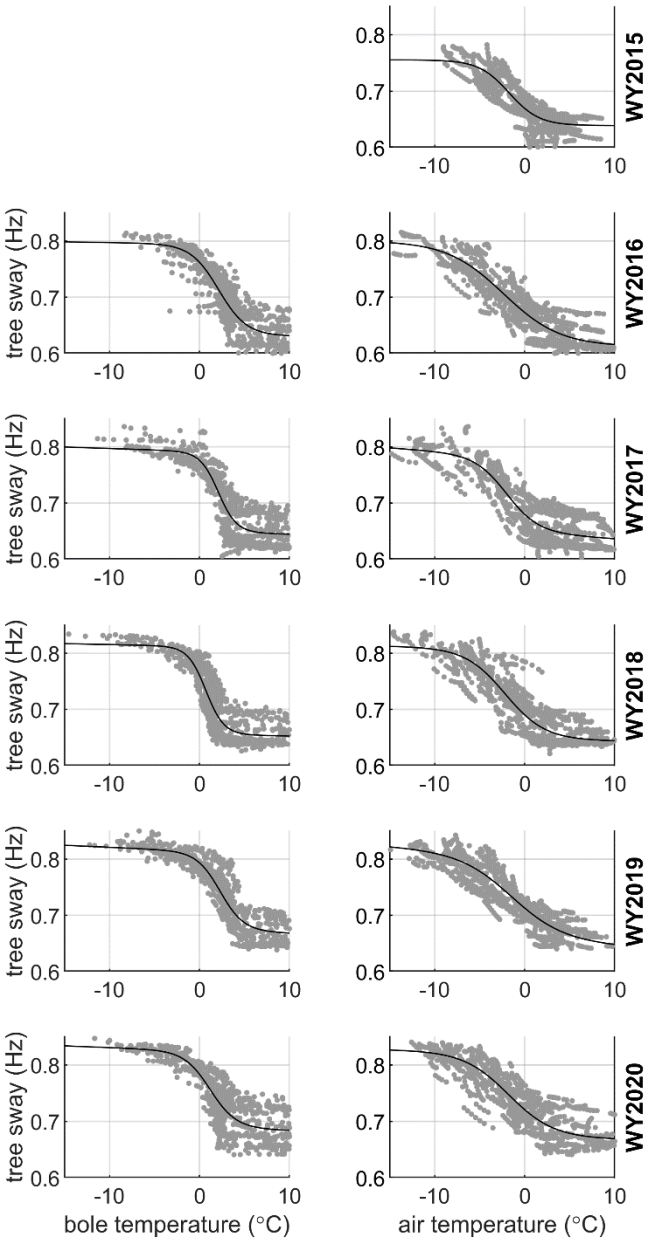

Figure S10. Same as Figure S9 but for the Niwot fir tree.

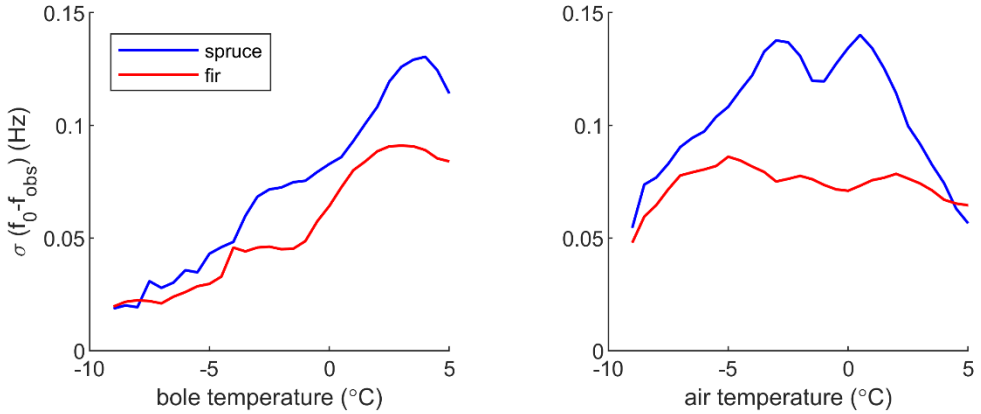

172

173 **Figure S11.** Standard deviation in the residuals ($f_0 - f_{obs}$) of the Equation 4 fit across all years,
174 versus (left) bole temperatures and (right) 36-hr smoothed air temperatures for the spruce
175 (blue) and fir (red). Values are computed over a sliding 2°C window.

176

177

178 **Table S1.** Characteristics of trees instrumented with accelerometers (DBH = diameter at breast
179 height). Tree characteristics were measured in summer 2017.

Species	DBH (cm)	Crown dia. (m)	Canopy bottom height (m)	Tree Height (m)	Accelerometer Height (m)
Engelmann spruce	35.7	3.4	2.8	13.0	8.9
Subalpine fir	18.5	1.7	2.3	11.0	8.1

180

181 **Table S2.** Parameters fit to Equation 4 for the spruce tree each year, reported separately for
182 the bole and 36-hr smoothed air temperature datasets, along with fit statistics.

Water year	Temperature source	Curve parameters					Statistics	
		a	*b*	*c*	*d*	*h*	R^2	*RMSE (Hz)*
2015	bole	--	--	--	--	--	--	--
	air	1.016	0.6245	1.209	0.3236	0.00187	0.793	0.037
2016	bole	0.9831	0.5889	1.258	-1.773	0.000226	0.894	0.032
	air	0.9637	0.3463	1.266	0.4744	2.22e-14	0.880	0.033
2017	bole	0.9965	1.007	1.233	-2.292	0.00139	0.890	0.032
	air	0.9919	0.5569	1.224	1.088	0.00166	0.874	0.033
2018	bole	0.9895	1.039	1.223	-1.287	0.00161	0.881	0.033
	air	0.9772	0.5538	1.217	0.6826	0.00125	0.899	0.030
2019	bole	0.9970	0.7393	1.237	-2.263	0.00206	0.947	0.023
	air	0.9858	0.5053	1.214	0.2634	0.00280	0.916	0.029
2020	bole	0.9791	0.6639	1.237	-1.262	0.000371	0.919	0.027
	air	0.9715	0.4841	1.233	0.5358	0.000553	0.925	0.027

183 **Table S3.** Same as Table S2 but for the fir tree.

Water year	Temperature source	Curve parameters					Statistics	
		a	*b*	*c*	*d*	*h*	R^2	*RMSE (Hz)*
2015	bole	--	--	--	--	--	--	--
	air	0.6389	0.5944	0.7553	1.035	2.22e-14	0.761	0.021
2016	bole	0.6329	0.6459	0.7947	-1.374	0.000236	0.785	0.026
	air	0.6122	0.3161	0.8002	0.7431	2.22e-14	0.805	0.025
2017	bole	0.6497	0.9917	0.7918	-2.076	0.000522	0.750	0.029
	air	0.6476	0.5655	0.7813	1.138	0.00113	0.756	0.029
2018	bole	0.6558	0.9983	0.8119	-0.7124	0.000324	0.794	0.026
	air	0.6459	0.4509	0.8088	0.9856	0.000245	0.836	0.024
2019	bole	0.6750	0.7649	0.8137	-1.754	0.000712	0.868	0.021
	air	0.6565	0.3489	0.8063	0.5048	0.00111	0.848	0.022
2020	bole	0.6898	0.6943	0.8248	-0.8224	0.000611	0.720	0.029
	air	0.6705	0.3990	0.8237	0.7126	0.000237	0.768	0.027

184 **Table S4.** Parameters fit to Equation 7 for the two study trees, along with fit statistics.

Study tree	n	**α parameter (kg Hz^{-1} Δ*f*)** (95% confidence intervals)	Statistics	
			R^2	*RMSE (kg Hz^{-1} Δf)*
spruce	12	**1092.4** (970.1, 1215)	0.801	6.3
fir	18	**321.9** (330.6, 343.3)	0.918	4.1

185